Proceedings of the 17th World Congress
The International Federation of Automatic Control
Seoul, Korea, July 6-11, 2008

# An Adaptive Sub-Optimal Energy Management Strategy for Hybrid Drive-Trains

**Thijs van Keulen,** * **Bram de Jager, Maarten Steinbuch**

* *Technische Universiteit Eindhoven, P.O. BOX 513, 5600 MB, Eindhoven, The Netherlands (Tel: +31 40 247 4828; e-mail: t.a.c.v.keulen@tue.nl).*

**Abstract:** Typically the energy management problem of a hybrid vehicle is formulated as an optimization problem, where the optimal power split between the prime mover and the secondary power converter is calculated off line based on a given driving cycle and solved numerically with dynamic programming techniques. An important constraint is that the energy level of the secondary power source at the end is the same as in the beginning. In real live the future driving cycle is not known a priori, making it difficult to calculate the exact optimal power split beforehand. To arrive at a practical real time control algorithm, a sub-optimal control law can be applied, where the end-point constraint is replaced by a term in the cost function that accounts for the change in energy; in case of a hybrid electric vehicle it represents the fuel equivalence of the stored reversible energy. In this paper it is reasoned that the reversible energy contains also kinetic and potential energy of the vehicle as well as energy stored in the secondary power source. By feedback control of the state of energy of the secondary power source, the amount of stored energy can be kept on a trajectory, such that the total amount of reversible energy remains constant. Kinetic and potential energy is proportional with vehicle mass, therefore this trajectory is adaptive to vehicle loading. In this paper simulations of an on-line strategy are included that show fuel consumption improvements of a distribution truck, close to those obtained with dynamic programming, validating the reasoning.

## 1. INTRODUCTION

Hybridization of drive-trains is an often proposed method for fuel consumption reduction in vehicles. A hybrid vehicle contains two power converters instead of one. Main advantage of hybrid vehicles is that kinetic energy can be recovered and stored, such that it can be used at a later, more convenient, time to propel the vehicle. The use of the stored energy is governed by the energy management strategy (EMS).

EMS for hybrid drive-trains are control algorithms that split the power request between the two power converters. During the past years, several contributions have been made regarding energy management of hybrid vehicles, see, e.g., Sciarretta and Guzzella [2007] for an overview. One of the possibilities to arrive at a real time algorithm is to express the stored battery energy in an equivalent amount of fuel, see Guzzella and Sciarretta, [2005, pages 199-201], Rodatz et al. [2005], Johnson et al. [2000], Lin et al. [2003] and Koot et al. [2005]. In these strategies changes in properties of the vehicle have not been included.

This paper considers aspects that are particularly relevant for trucks. Trucks differ from passenger cars in the large variability in vehicle mass; a truck can be loaded or unloaded changing its mass by a factor of $2 - 2.5$ for distribution trucks. The main contribution of this paper is an EMS that includes the vehicle kinetic and potential energy and therefore is adaptive to vehicle mass.

The paper is organized as follows; first a hybrid vehicle model will be discussed, secondly an EMS is suggested, in the third part the proposed strategy is evaluated in a simulation environment, finally conclusions are included.

## 2. VEHICLE MODEL

The vehicle considered in this paper is a medium duty, parallel hybrid electric, distribution truck. The use of a distribution truck is characterized by frequent start-stop behavior. The prime mover of the truck is a diesel engine, while the secondary power converter is an electric machine supplied by a battery pack as storage device. The diesel engine has a maximum power of 136 kW, and the maximum power of the electric machine is 44 kW. The lithium-ion battery used has a maximum capacity of 9 MJ.

The topology of the drive-train components in a parallel hybrid configuration can be schematically viewed in Fig. 1. The rotating speed of the electric machine is equal to the engine speed. The driver of the truck can pose a power request. The vehicle model takes into account the vehicle longitudinal dynamics, the diesel engine, electric machine and battery.

* Thijs van Keulen would like to thank Michiel Koot and Guus Arts for the use of their simulation toolkit.

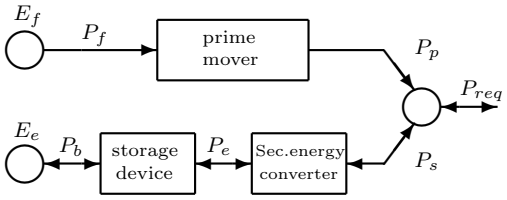


Fig. 1. Drive train topology.

### 2.1 Vehicle Longitudinal Dynamics

The longitudinal vehicle dynamics are modeled with a single body.

$$T_p + T_s = \left( F_{rl} + m\frac{dv}{dt} \right) R_e \tag{1}$$

$$F_{rl} = c_2 v^2 + c_1 v + c_0 \tag{2}$$

Here $m$ is the effective vehicle mass, including the inertia of the rotating parts, $R_e$ the effective rolling radius of the wheels, $T_p$ is the torque delivered by the engine, $T_s$ is the torque delivered by the electric machine and $F_{rl}$ is the road load force of the vehicle. It is assumed that the road load force of the vehicle $F_{rl}$ is described by a second order function of the vehicle speed $v$. The parameters can be derived during coast down measurements and are related to aerodynamic drag $c_2$ and roll and friction losses $c_1$, $c_0$.

The gear shift strategy of the vehicle is not considerate; the gear and clutch position are set a priori, thereby prescribing the engine and electric machine speed $\omega$. The dependence of rolling resistance to vehicle mass is neglected.

### 2.2 Diesel Engine

The engine is modeled by a non-linear static map, see Fig. 2, relating the engine torque $T_p$ and rotational speed $\omega$ to fuel rate. For any engine speed $\omega$ there is a maximum torque that can be delivered, shown by the maximum torque line. The Drag Torque line shows the drag torque $T_{drag}$ the engine consumes during coasting. Using the exhaust brake this torque can be increased, see the Exhaust Brake Torque line. Normally the exhaust brake is applied going down hill to prevent the normal brake system from overheating.

### 2.3 Electric Machine

The electric machine is also modeled by a non-linear static map, relating the electric machine torque $T_s$ and rotational speed $\omega$ to a conversion efficiency, see Fig. 3. The electric machine can work both as a motor and as a generator. At low rotational speeds the electric machine is limited by maximum torque, while at higher speeds the electric machine is limited by maximum power.

### 2.4 Battery

A battery has losses during charging and discharging. The losses during charging ($\approx 20\%$) differ from the losses

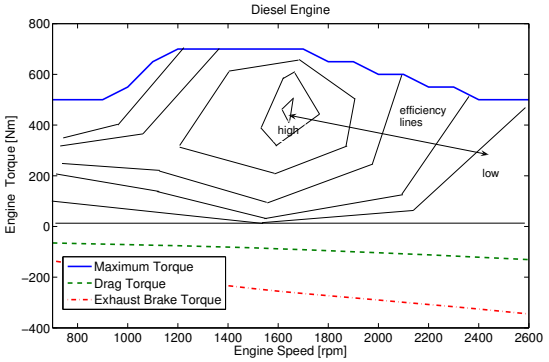


Fig. 2. Fuel Conversion Efficiency Map Diesel Engine.

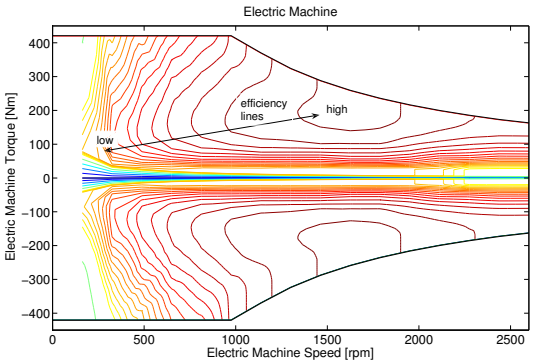


Fig. 3. Conversion Efficiency Map Electric Machine.

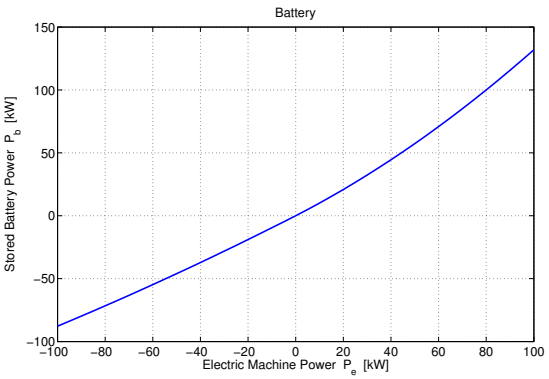


Fig. 4. Battery Efficiency Characteristic.

during discharging ($\approx 10\%$). The battery is described with a power based model, see Fig. 4. Thermal and transient effects are not considerated. The only state variable in the battery model is the energy $E_e(t)$. This is calculated by integrating the power flow $P_b$, which is defined as:

$$E_e(P_s, t) = E_e(0) + \int_0^\tau P_b(P_s, t)dt \tag{3}$$

The state of energy $SOE$ of the battery can be defined as the ratio between the current stored energy level $E_e(t)$ and the maximum storage capacity of the battery $E_{emax}$.

$$SOE = \frac{E_e}{E_{emax}} \tag{4}$$

## 3. ENERGY MANAGEMENT

The topology of the drive-train considered is depicted in Fig. 1. Here $P_{req}$ is the power request of the driver. It is assumed $P_{req}$ takes into account all vehicle and drive-train losses, including aerodynamic drag, rolling and friction losses. $P_p$ is the power delivered by the prime mover, while $P_s$ is the power delivered, or recuperated, by the secondary power converter. The total delivered power equals the requested power:

$$P_{req} = P_p + P_s \tag{5}$$

In practice the power converters are limited in power by a maximum value. The prime mover and the secondary power converter are characterized by non-linear functions of the vehicle operating conditions, e.g. shaft speed and delivered power. In case of a combustion engine as prime mover, energy recuperation is impossible.

The energy management has the freedom to split the power request over the prime mover and the secondary power converter. The power delivered by the secondary power converter can be defined as the control variable $x = P_s$ in the energy management control problem. The consumed energy of the prime mover $E_f$ as well as the consumed energy of the secondary power converter $E_e$, can be calculated by integrating the consumed powers $P_f$ and $P_b$ over the elapsed time.

$$E_f = \int_0^{t_f} P_f(x,t)dt \tag{6}$$

$$E_e = \int_0^{t_f} P_b(x,t)dt \tag{7}$$

Objective of the energy management is to minimize the total energy consumption of the vehicle by adjusting the power split ratio $x$ in an optimal way in time.

$$J(x,t_f) = E_f + E_e \tag{8}$$

$$\min_x J(x,t_f) = \min_x \left( \int_0^{t_f} P_f(x,t)dt + \int_0^{t_f} P_b(x,t)dt \right) \tag{9}$$

To make a "fair" comparison with a conventional drive train, $SOE$ of the secondary power source $E_e(t)$ is equal at the end of the cycle to the energy level at the beginning. This is often referred to as the end-point constraint.

$$SOE(0) \quad = \quad SOE(t_f) \quad \rightarrow \quad \int_0^{t_f} P_b(x,t)dt = 0 \quad \text{so,}$$

$$\min_x J(x,t_f) = \min_x \left( \int_0^{t_f} P_f(x,t)dt \right) \quad \text{sub} \left( \int_0^{t_f} P_b(x,t)dt = 0 \right) \tag{10}$$

To minimize the function $J(x,t_f)$ subject to the end-point constraint, the method of Lagrange multipliers can be applied.

$$\min_{x,\lambda} \bar{J}(x,t_f) = \min_{x,\lambda} \left( \int_0^{t_f} P_f(x,t)dt + \lambda \int_0^{t_f} P_b(x,t)dt \right) \tag{11}$$

Here $\lambda$ is a Lagrange multiplier. The Lagrange multiplier has a physical interpretation, it represents the relative incremental cost of the prime mover and secondary power converter. The minimization can be obtained by solving (11) for $x$ and $\lambda$.

Choosing a certain driving cycle Dynamic Programming (DP) techniques can compute the optimal $\lambda$ and $x(t)$ for this particular driving cycle. Note that the achievable fuel consumption reduction is drive cycle dependent, as is the optimal trajectory. The exact future driving cycle is not known in advance, and therefore $\lambda_{opt}$ is not known either. One way to deal with this is to replace $\lambda$ by a term in the cost function that expresses the stored energy in a fuel equivalence value $s(t)$, that is controlled by the EMS. This will simplify the optimization problem (11) to an optimization only depending on the vehicular parameters at the current time. These strategies are often referred to as Equivalent Consumption Minimization Strategies (ECMS), see, e.g., Guzzella and Sciarretta, [2005, pages 199-201].

It was already stated that the drive-train component characteristics are non-linear functions of the vehicle operating conditions. It can be expected that $s$ will vary under different conditions. If the initial $s$ is chosen too high the battery will over charge over the long run, while a too small $s$ will deplete the battery. To prevent the secondary power source from depleting or overcharging , several algorithms are suggested to adapt $s$ in real time for the current driving conditions, see Guzzella and Sciarretta, [2005, pages 199-201], Koot et al. [2005], Rodatz et al. [2005] or Sciarretta and Guzzella [2007]. In Koot et al. [2005] the equivalence factor is chosen to be an affine function of the current state of energy, with proportional feedback gain $K$.

$$s(t) = s_0 + K\left(E_{e0} - E_e(t)\right) \tag{12}$$

Here $E_e(t)$ is the current state of energy, and $E_{e0}$ forms a set-point for the battery state of energy, $K$ will control $E_e(t)$ towards $E_{e0}$. $s_0$ and $K$ can be tuned for a certain drive cycle and vehicle configuration, and than show energy consumption rates very close to those obtained with DP. However in simulations it can be noticed that $\lambda_{opt}$, for charge sustainability, will vary substantially for different vehicle masses, see Fig. A.1 and A.2. A larger vehicle mass requires a higher power demand. The characteristics of the engine, motor and battery are a function of the power flowing through the devices; therefore the vehicle mass has influence on the optimal fuel equivalence factor $s$.

In Rodatz et al. [2005] it is correctly observed that the vehicle itself, like the battery, is a reversible energy storage system; therefore we propose to include the kinetic and potential energy in the reversible energy. In real time it is possible to calculate the current kinetic and potential energy of the vehicle (the vehicle mass can be estimated with an observer). It makes use of the fact that the kinetic and potential energy is proportional with the vehicle mass

at a certain velocity, in this way the control algorithm will be adaptive to vehicle loading.

Not all kinetic and potential energy can be recovered, a part of it will be dissipated during braking. Nevertheless, assuming an average deceleration rate $\hat{a}$, it is possible to make an estimation of the amount of brake power required $\hat{P}_{br}$, to stop the vehicle from a current velocity $v_0(t)$.

$$\hat{P}_{br}(t,\tau) = (m\hat{a} + mg\sin\hat{\alpha})\,\hat{v}(t,\tau) \tag{13}$$

Here $\hat{v}(t,\tau)$ is the expected velocity path, $m$ is the vehicle mass, $g$ is the gravitational constant, and $\hat{\alpha}$ is the expected road angle. The "hat" indicates variables estimated.

We believe the constant deceleration assumption can be justified, as the braking behavior of trucks is better predictable than that of passenger cars. During deceleration, part of the deceleration will be due to the aerodynamic drag force and the rolling resistance of the tires, forces lumped in the road load force $F_{rl}$, see (2). For the expected velocity path $\hat{v}(\tau)$, the power losses due to road load forces during the deceleration is described by a third order polynomial of the expected velocity path $\hat{v}(t,\tau)$.

$$\hat{P}_{rl}(t,\tau) = F_{rl}(t,\tau)\hat{v}(t,\tau) \tag{14}$$

$$= c_2\hat{v}(t,\tau)^3 + c_1\hat{v}(t,\tau)^2 + c_0\hat{v}(t,\tau) \tag{15}$$

The expected additional required brake power is given by the difference between the required brake power $\hat{P}_{br}(t,\tau)$ and the road load power $\hat{P}_{rl}(t,\tau)$ and possibly the engine drag power $\hat{P}_{drag}$, when the clutch is engaged. This brake power is delivered by the generator until the maximum generator power $P_{genmax}$ is reached, the rest of the brake power is absorbed by the brake system. The expected recoverable brake power in time $\hat{P}_r(t,\tau)$ can be calculated.

$$\hat{P}_r(t,\tau) = \max(0, \min(P_{genmax}, \hat{P}_{br} - \hat{P}_{rl} - \hat{P}_{drag})) \tag{16}$$

The expected future recoverable electric energy $\hat{E}_r(t)$ can be estimated by integrating $\hat{P}_r(t,\tau)$ over the estimated stop time $\hat{t}_{stop}$, hereby not exceeding the maximum battery capacity $E_{cap}$.

$$\hat{E}_r(t) = \min\left(\int_0^{\hat{t}_{stop}} \hat{P}_r(t,\tau)d\tau, E_{cap}\right) \tag{17}$$

$\hat{E}_r(t)$ can be included in (12), leading to:

$$s(t) = s_0 + K\left[\left(E_{e0} - \hat{E}_r(t)\right) - E_e(t)\right] \tag{18}$$

In this EMS, the battery set-point $E_{e0}$ is adjusted by the future recoverable energy $\hat{E}_r$. Feedback gain $K$ controls the battery state of energy towards the adaptive set-point $(E_{e0} - \hat{E}_r)$. The advantage is that the control algorithm allows for deeper discharge when the vehicle drives faster, drives uphill or has a larger mass. For $E_{e0}$ a value close to the maximum capacity of the battery can be chosen.

## 4. SIMULATION RESULTS

### *4.1 Drive Cycle*

The Federal Test Procedure-75 (FTP-75) for city cycle testing is considered, see SAE J1506 [2002]. Fig. 5 shows the FTP-75 drive cycle with several start-stop movements. Based upon the vehicle mass, road load properties, aerodynamic drag and rolling resistance, the required drive power $P_{req}$ to follow the drive cycle velocities can be calculated. One remark can be made; it is now required that a loaded truck drives exactly the same speed profile as the empty truck, while in practice a driver will accept that a loaded truck accelerates slower.

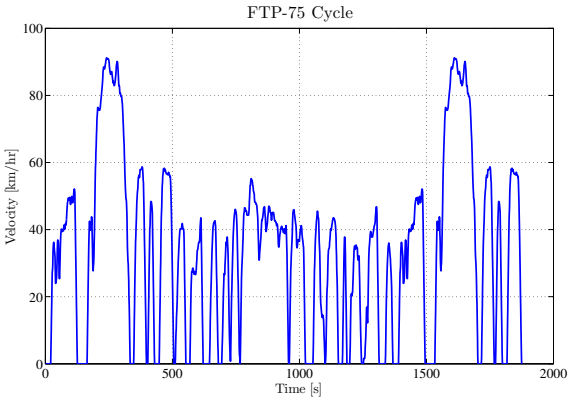


Fig. 5. FTP-75 Drive Cycle.

### *4.2 Base-Line Vehicle*

To illustrate the fuel reduction potential of a hybrid drive-train, it can be compared with a base line vehicle, which uses only the combustion engine of section 2.2 for propulsion, so $P_s = 0$. The fuel consumption of the empty and loaded base line truck can be seen in Table A.1.

### *4.3 Dynamic Programming*

The non-linear optimization problem (11) for the hybrid truck of section 2, can be solved with DP techniques. The results are shown in Table A.1, and Fig. A.3 and A.6. Fig. A.3 shows the optimal trajectory of $SOE$ over the FTP-75 cycle. Results of the empty and loaded truck are shown, clearly vehicle mass has influence on the optimal trajectory. Fig. A.6 shows the Lagrange multiplier $\lambda_{opt}$, if the truck is loaded, $\lambda_{opt}$ becomes smaller. The fuel reduction potential of the empty hybrid truck is 14.5 %, while for the fully loaded truck it is 10.4 %. The reduction potential of the loaded truck is lower than the empty truck, as the electric machine power is relatively small and therefore the part of the kinetic energy that can be recovered is limited. The DP results form a benchmark for the proposed real time control strategy.

### *4.4 On-line EMS*

To illustrate the value of including the recoverable energy in the EMS, both feedback algorithm (12) and (18) are simulated. Based upon real life driving behavior, the

expected deceleration rate $\hat{a}$ used in the simulations was 0.7 m/s$^2$. The control settings for both (12) and (18) are $E_{e0} = 50\%$, $s_0 = 2.7$ and $K = 10^{-6}$. Note that this is not necessarily the optimal setting for (18). Furthermore the end-point constraint of (10) is not fulfilled. The $\Delta SOE$ is expressed in an equivalent amount of fuel, using $\lambda_{opt}$ derived with DP and a diesel heating value of 43 MJ/kg. The fuel potential results are shown in Table A.1, the equivalent fuel consumption is placed between brackets. The adaptive feedback algorithm shows a fuel reduction that is better than with feedback without adaptation and is close to the optimum obtained with DP.

Fig. A.4 and A.5 show the $SOE$ trajectory obtained with the EMS. The optimal trajectory is better followed when $E_r$ is included, in particular with the loaded truck at time interval the point in the cycle where the speed is 90 km/hr. Fig. A.4 and A.5 show the fuel equivalence value $s$. In case $E_r = 0$, Fig. A.7 is a inverted and scaled version of Fig. A.4. The average adapted equivalence value $s$ is smaller for the loaded truck, in agreement with Fig. A.6.

## 5. CONCLUSIONS

In this paper the future recoverable energy is estimated assuming the vehicle will decelerate by a certain average deceleration. Using the future recoverable energy, an adaptive battery state of energy set-point is determined. A feedback loop is added to control the battery state of energy towards the set-point and prevent the battery from depleting. Simulations show that the new control law obtains a performance, at different vehicle masses, close to the optimum obtained with DP.

The EMS can be made adaptive to driver behavior by adjusting the deceleration rate in real time. Verification of the control algorithm is scheduled on the Eindhoven University of Technology chassis dynamometer.

## REFERENCES

L. Guzzella and A. Sciarretta. Vehicle Propulsion Systems. Introduction to Modeling and Optimization. Berlin: Springer-Verlag, 2005.

V.H. Johnson, K. Wipke, and D. Rausen. HEV Control Strategy for Real-Time Optimization of Fuel Economy and Emissions. *Proc. SAE*, Paper 2000-01-1543, 2000.

Society of Automotive Engineers. J1506 Emission Test Driving Schedules. *SAE Standard*, 2002.

M. Koot, J. Kessels, B. de Jager, W. Heemels, P. van den Bosch, M. Steinbuch. Energy Management Strategies for Vehicular Electric Power Systems. *IEEE Transactions On Vehicular Technology*, Vol. 54, No. 3, pages 771-782, May 2005.

M. Koot, J. Kessels, B. de Jager, P. van den Bosch. Fuel reduction potential of energy management for vehicular electric power systems. *Int. J. Alternative Propulsion*, Vol. 1, No. 1, pages 112-131, 2006.

C. C. Lin, H. Peng, J. W. Grizzle, J. M. Kang. Power Management Strategy for a Parallel Hybrid Electic Truck. *IEEE Transactions on Control Systems Technology*, Vol. 11, No. 6, pages 839-849, 2003.

A. Sciarretta, L. Guzzella. Control of Hybrid Electric Vehicles. *IEEE Control Systems Magazine*, April 2007.

P. Rodatz, G. Paganelli, A. Sciarretta, L. Guzzella. Optimal power management of an experimental fuel cell/supercapacitor-powered hybrid vehicle. *Control Engineering Practice*, Vol. 13, pages 41-53, 2005.

## Appendix A. TABLES AND FIGURES

Table A.1. Fuel Consumption Results

| Simulation Results | | | |
|---|---|---|---|
| Strategy | Fuel cons. [g] | [1/100 km] | reduction [%] |
| Empty truck 9000 kg | | | |
| BL | 3373 | 22.8 | - |
| DP | 2860 | 19.3 | 14.5 |
| RT | 2959 (2955) | 20.0 (20.0) | 12.3 (12.4) |
| RT-ADAPT | 2930 (2947) | 19.8 (19.9) | 13.1 (12.6) |
| Loaded truck 18000 kg | | | |
| BL | 5753 | 39.4 | - |
| DP | 5156 | 35.4 | 10.4 |
| RT | 5209 (5172) | 35.7 (35.4) | 9.5 (10.1) |
| RT-ADAPT | 5165 (5166) | 35.4 (35.4) | 10.2 (10.2) |

BL=Base Line vehicle, DP are the dynamic programming results, RT are the results of the feedback loop without the recoverable energy estimation, and RT-ADAPT are the results of the proposed on-line energy management strategy.

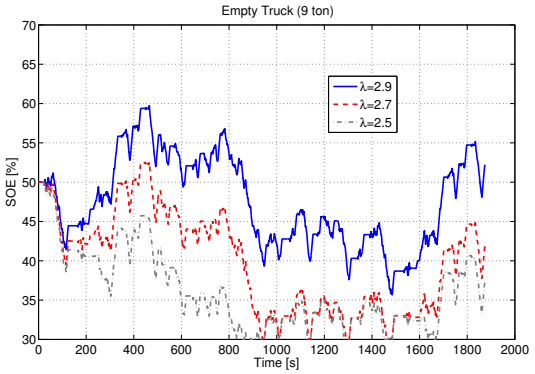


Fig. A.1. $SOE$ during FTP-75 cycle for an empty truck.

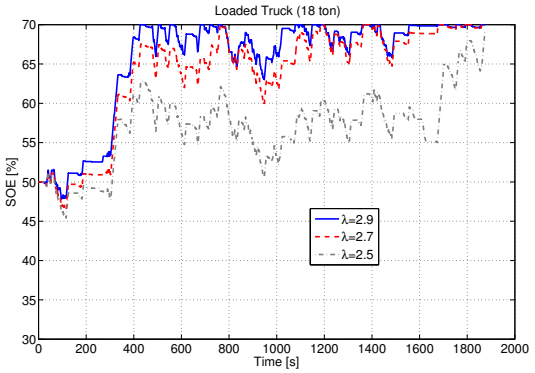


Fig. A.2. $SOE$ during FTP-75 cycle for a loaded truck.

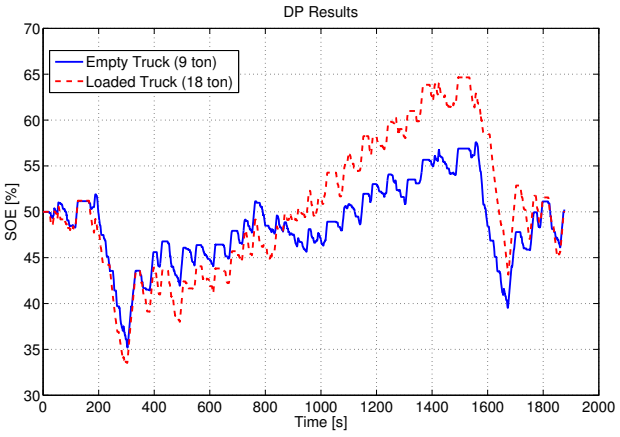


Fig. A.3. Optimal $SOE$ during FTP-75 cycle for an empty and a loaded truck.

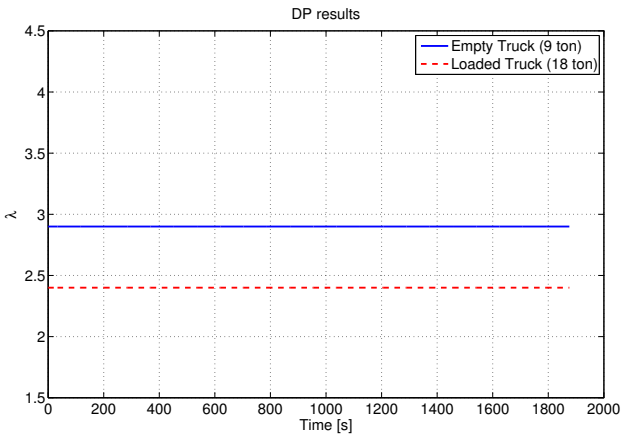


Fig. A.6. $\lambda_{opt}$ during FTP-75 cycle for an empty and a loaded truck.

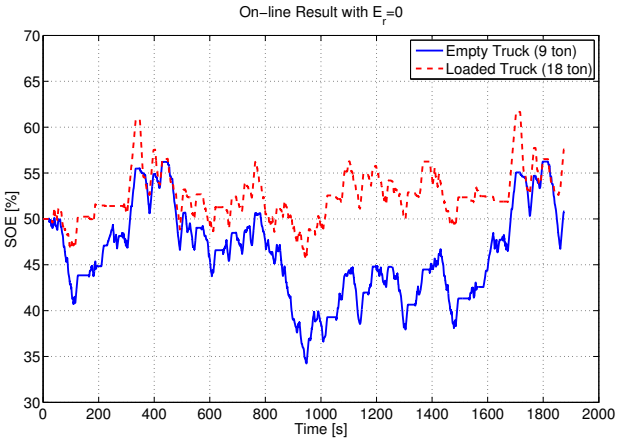


Fig. A.4. On-line results without recoverable energy estimation; $SOE$ during FTP-75 cycle for an empty and a loaded truck.

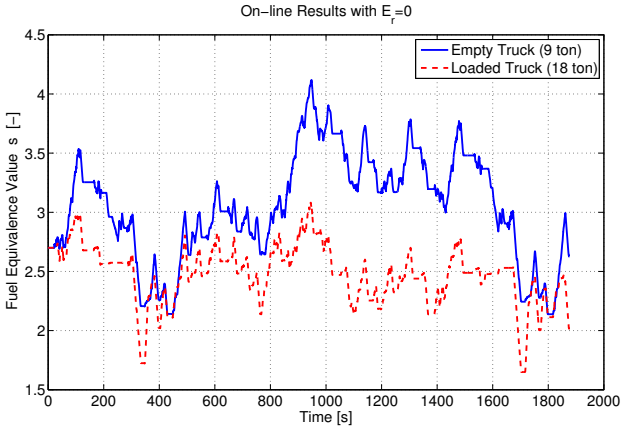


Fig. A.7. On-line results without recoverable energy estimation; $s$ during FTP-75 cycle for an empty and a loaded truck.

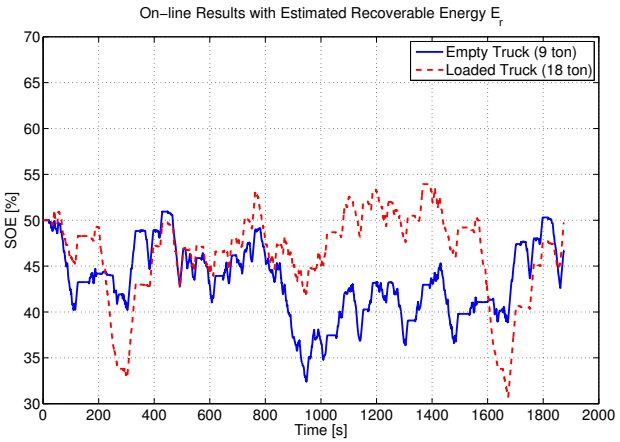


Fig. A.5. On-line results with recoverable energy estimation; $SOE$ during FTP-75 cycle for an empty and a loaded truck.

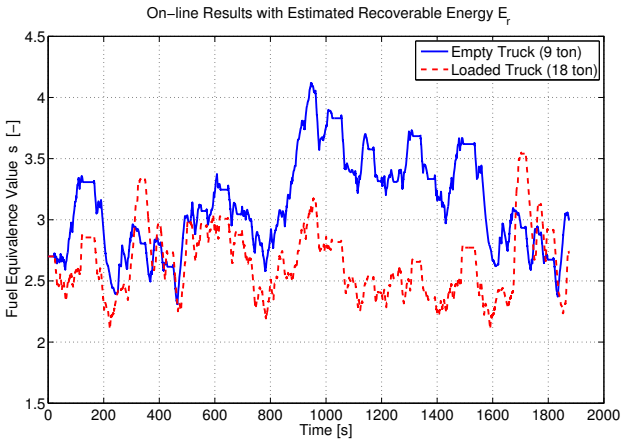


Fig. A.8. On-line results with recoverable energy estimation; $s$ during FTP-75 cycle for an empty and a loaded truck.